IEEE Photonics Journal
An IEEE Photonics Society Publication

Open Access

Optical Frequency Shifter Employing a Brillouin-Assisted Filtering Technique

Volume 9, Number 2, April 2017

Hao Chen
Erwin H. W. Chan, *Senior Member, IEEE*

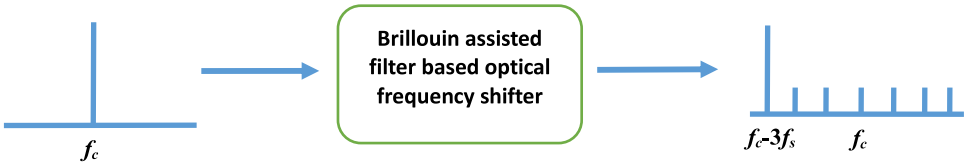

DOI: 10.1109/JPHOT.2017.2688441
1943-0655 © 2017 IEEE

IEEE photonics SOCIETY

IEEE

Optical Frequency Shifter Employing a Brillouin-Assisted Filtering Technique

Hao Chen and Erwin H. W. Chan, ***Senior Member, IEEE***

School of Engineering and Information Technology, Charles Darwin University, Darwin, NT 0909, Australia

DOI:10.1109/JPHOT.2017.2688441

Manuscript received March 6, 2017; accepted March 23, 2017. Date of publication March 29, 2017; date of current version April 12, 2017. Corresponding author: Erwin H. W. Chan (e-mail: erwin.chan@cdu.edu.au).

Abstract: A new optical frequency shifter is presented. It is based on a double sideband suppressed carrier radio-frequency (RF) modulated optical signal into a Brillouin-assisted filter, which is formed by a Brillouin medium between a pair of optical circulators. The frequency shifting operation is realized by utilizing multiple stimulated Brillouin scattering gain and loss spectra to amplify one of the third-order sidebands but attenuate the other sidebands. The frequency shifter has a simple structure and a high frequency shifted to unwanted frequency component ratio. It also has the ability to realize a very large frequency shift, which is three times the input electrical driving signal frequency. The frequency shifter is experimentally demonstrated with the results showing a 32.53 GHz optical frequency shift of a continuous wave light at 1551.016 nm with over 34 dB difference between the wanted frequency shifted and unwanted frequency components.

Index Terms: Fiber optics systems, microwave photonics signal processing, electro-optical systems.

1. Introduction

Translating a continuous wave light from one frequency into another has been a subject of interest for more than 30 years. It has applications including gyroscopes, heterodyned sensors, spectroscopy, signal processing, and coherent communication [1], [2]. Various techniques have been reported to shift the light frequency. An acousto-optic frequency shifter can be implemented by using fiber mode coupling inside a fiber or acousto-optic effect in a Bragg cell [3]. Serrodyne frequency translation is another technique for shifting the light frequency. In this case, optical frequency shifting is realized by phase modulating a continuous wave light with an electrical sawtooth [2]. However, only a small frequency shift of few GHz can be obtained using the above techniques. Techniques including using coupled inverted slot lines integrated on an X-cut $LiNbO_3$ substrate [4], using a dual-electrode traveling wave modulator inside a Sagnac fiber loop interferometer [5], using a dual-parallel Mach Zehnder modulator (MZM) [6] and using stimulated Brillouin scattering (SBS) in an optical fiber [7] have been reported to obtain a large frequency shift of more than 10 GHz. However, they either rely on electrical components, have a complex structure that involves two modulators and/or two microwave signal generators, or generate high unwanted frequency components. Furthermore, all the above frequency shifting techniques require an input electrical driving signal with the frequency equal to the frequency shift. Hence a large frequency shift requires a high frequency microwave signal generator.

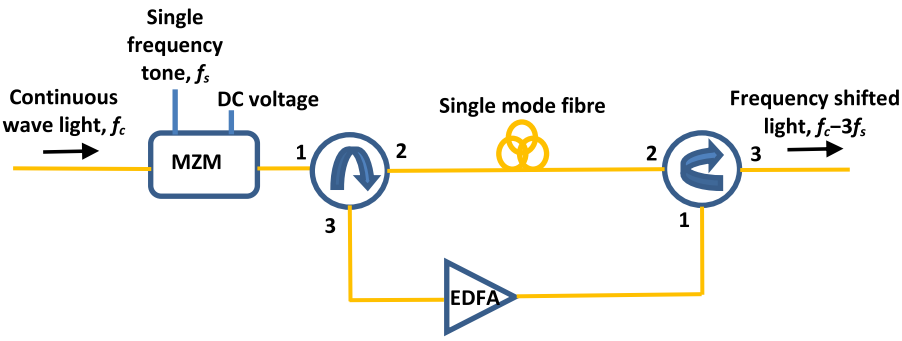

Fig. 1. Optical frequency shifter structure.

This paper presents a new optical frequency shifter based on a Brillouin assisted filtering technique. The frequency of the input electrical driving signal only needs to be one third of the frequency shift. The new optical frequency shifter has a simple structure that involves a single MZM and off-the-shelf optical components. Different frequency shift can be obtained by tuning the laser source wavelength or using different Brillouin medium. Experimental results are presented that demonstrate a large frequency shift of 32.53 GHz using an electrical driving signal having 10.842 GHz frequency into an MZM and a high frequency shifted to unwanted frequency component ratio of over 34 dB.

2. Frequency Shifter Operation Principle and Analysis

The structure of the optical frequency shifter is shown in Fig. 1. The optical carrier from the laser source is modulated by a MZM driven by a single frequency tone with the frequency f_s. The MZM is biased at the minimum transmission point, which suppresses the optical carrier and the even order sidebands at the MZM output leaving the odd order sidebands [8]. Hence the output of the MZM is a double sideband suppressed carrier (DSB-SC) RF modulated optical signal and its electric field can be written as

$$E_{MZM}(t) = E_{in}\sqrt{t_{ff}}\left[J_1(\beta_s)\cos((\omega_c \pm \omega_s)t) - J_3(\beta_s)\cos((\omega_c \pm 3\omega_s)t)\right] \quad (1)$$

where E_{in} is the laser electric field amplitude, t_{ff} is the MZM insertion loss, $J_n(x)$ is the Bessel function of n^{th} order of first kind, $\omega_c = 2\pi f_c$ is the carrier angular frequency, $\omega_s = 2\pi f_s$ is the single tone angular frequency, $\beta_s = \pi V_s/V_\pi$ is the modulation index, V_s is the voltage of the single frequency tone into the MZM, and V_π is the modulator switching voltage. Note that the power of the n^{th} order sideband is proportional to $J_n(\beta_s)^2$. Simulation results show the fifth and the higher order sidebands are $>$25 dB below the 3rd order sideband for a modulation index $\beta_s < 2$. Hence, they are neglected in (1).

The MZM output power spectral density is the Fourier transform of the autocorrelation of the electric field [9] and is given by

$$S_{MZM}(\omega) = \pi P_{in} t_{ff}\left[{J_1}^2(\beta_s)\,\delta\{\omega + \omega_c \pm \omega_s\} + {J_3}^2(\beta_s)\,\delta\{\omega + \omega_c \pm 3\omega_s\}\right] \quad (2)$$

where P_{in} is the laser output optical power, and $\delta\{\}$ represents a delta function. The output of the MZM, which consists of the fundamental and third order sidebands, is launched into a Brillouin assisted filtering structure [10]. The Brillouin assisted filter is formed by a single mode fiber, which is used as a Brillouin medium for SBS, between a pair of optical circulators. The single mode fiber has an SBS frequency f_{SBS}. Note that Port 3 of the first circulator is connected to Port 1 of the second circulator via an erbium-doped fiber amplifier (EDFA), which is used to amplify the backward traveling wave.

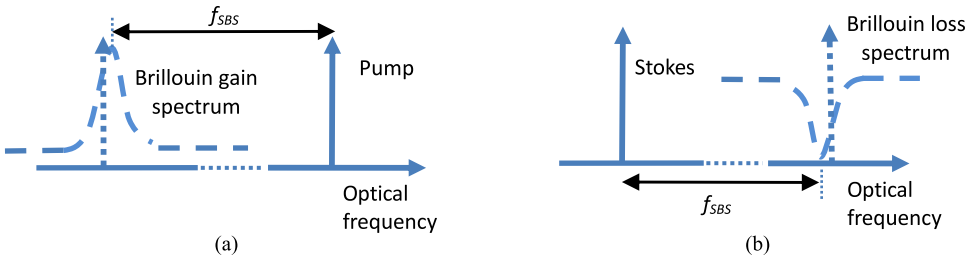

Fig. 2. Generation of a Brillouin (a) gain and (b) loss spectrum due to SBS interaction between a pump wave and a Stokes wave.

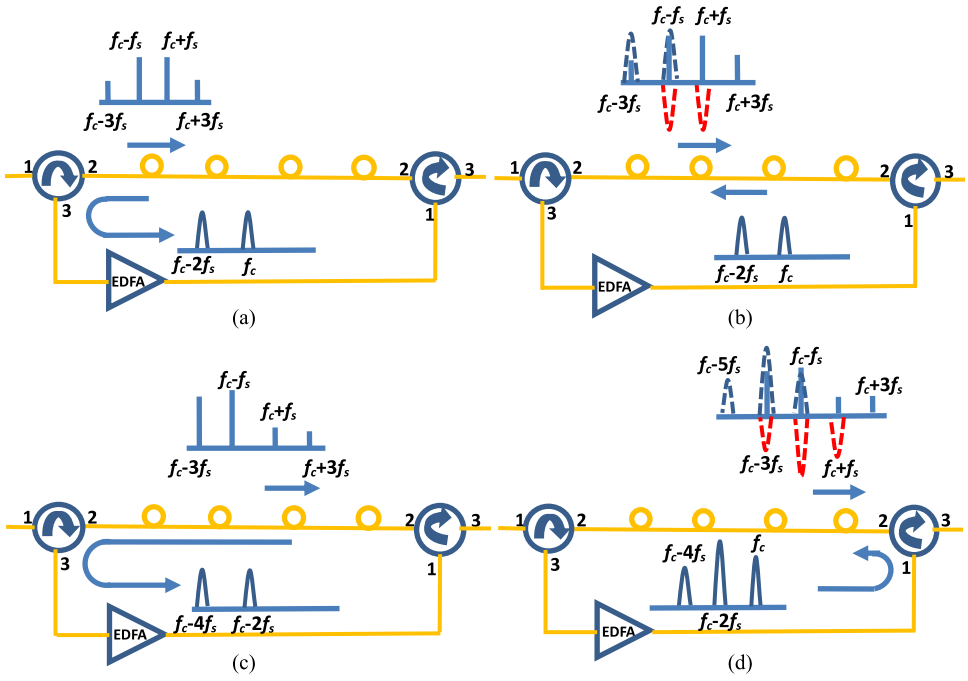

Fig. 3. Signals propagating inside a Brillouin assisted filter.

The single frequency tone into the MZM is designed to have the same frequency as the single mode fiber SBS frequency, i.e. $f_s = f_{SBS}$. In this case, different RF modulation sidebands at the MZM output can be amplified or attenuated due to the SBS effect as they passed through the Brillouin assisted filter. Fig. 2 summarizes the effect of SBS as two counter-propagating waves traveled through an optical fiber [11]. When a pump wave is launched into an optical fiber, a Brillouin gain spectrum centered at a frequency down shifted by the Brillouin frequency f_{SBS} of the fiber is generated in the counter-propagating wave (Stokes wave) as shown by the dashed line in Fig. 2(a). The pump power depletes as it transfers energy to amplify the Stokes wave. The Stokes wave induces a Brillouin loss spectrum centered at a frequency up shifted by the Brillouin frequency f_{SBS} as shown by the dashed line in Fig. 2(b).

In order to explain how the Brillouin assisted filter can be used to shift the laser frequency, the single mode fiber that is used as a Brillouin medium inside the Brillouin assisted filter is divided into four sections as shown in Fig. 3. Each section of the fiber has a length L. The DSB-SC RF modulated optical signal passed through the first circulator into the first section of the fiber. It acts as a pump wave for the SBS process. The power of the fundamental sidebands at $f_c \pm f_s$ are designed by controlling the power of the single frequency tone into the MZM and the laser source

power to above the SBS threshold value of the single mode fiber inside the Brillouin assisted filter. This generates the backscattered Brillouin wave [12] at f_c and $f_c - 2f_s$ traveling in the backward direction as shown in Fig. 3(a). The amplitude and the spectral shape of the backscattered Brillouin wave are determined by the pump power and the Brillouin gain coefficient [13], [14]. The backward traveling wave also consists of the frequency components due to Rayleigh backscattering of the forward traveling wave, i.e., the DSB-SC RF modulated optical signal. However, the amplitudes of the Rayleigh backscattering components are much smaller than that of the backscattered Brillouin wave when the power of the fundamental sidebands is above the optical fiber SBS threshold value. Hence the Rayleigh backscattering components are neglected in the analysis. The backscattered Brillouin waves at f_c and $f_c - 2f_s$ having the same amplitude pass through the first circulator and amplify by an EDFA to above the optical fiber SBS threshold value. The amplified backscattered Brillouin wave acts as a pump wave in the second section of the fiber for the SBS process. This generates two sets of gain and loss spectrums in the forward Stokes wave as shown by the dashed lines in Fig. 3(b). Therefore, the power spectral density of the forward Stokes wave after passing through the second section of the fiber becomes

$$\begin{aligned} S_{forward}(\omega) = \pi P_{in} t_{ff} e^{-\alpha 2L} \Bigg[& {J_1}^2(\beta_s) \frac{1}{g_{B1,2\omega_s}(\omega_c - \omega_s)} g_{B1}(\omega_c - \omega_s)\, \delta(\omega + \omega_c - \omega_s) \\ & + {J_1}^2(\beta_s) \frac{1}{g_{B1}(\omega_c + \omega_s)} \delta(\omega + \omega_c + \omega_s) \\ & + {J_3}^2(\beta_s)\, g_{B1,2\omega_s}(\omega_c - 3\omega_s)\, \delta(\omega + \omega_c - 3\omega_s) \\ & + {J_3}^2(\beta_s)\, \delta(\omega + \omega_c + 3\omega_s) \Bigg] \end{aligned} \tag{3}$$

where α is the fiber loss coefficient, and $g_{B1}(\omega)$ and $g_{B1,2\omega s}(\omega)$ is the SBS gain spectrum [14] generated by the backscattered Brillouin wave at f_c and f_c-$2f_s$ into the second section of the fiber respectively. The inverse of $g_{B1,2\omega s}(\omega_c - \omega_s)$ and $g_{B1}(\omega_c + \omega_s)$ given in (3) represent the amount of attenuation at the center of the two SBS loss spectrums at $f_c - f_s$ and $f_c + f_s$ respectively. Since the two backscattered Brillouin waves at f_c and $f_c - 2f_s$ have the same amplitude because the amplitude of the two fundamental sidebands at the MZM output are the same, the peak value of the two SBS gain spectrums are the same, i.e. $g_{B1}(\omega_c - \omega_s) = g_{B1,2\omega s}(\omega_c - 3\omega_s)$. Therefore from (3) the attenuation due to the SBS loss spectrum compensates for the amplification due to the SBS gain spectrum [15] in the negative fundamental sideband at $f_c - f_s$. Hence the amplitude of the negative fundamental sideband remains almost the same after the second section of the fiber. On the other hand, the positive fundamental sideband is attenuated and the negative third order sideband is amplified by the SBS loss and gain spectrum respectively.

The two high-power frequency components in the forward Stokes wave at $f_c - f_s$ and $f_c - 3f_s$ launch into the third section of the fiber. This generates the backscattered Brillouin wave at $f_c - 2f_s$ and $f_c - 4f_s$ due to SBS as shown in Fig. 3(c). This backscattered Brillouin wave is combined with the backscattered Brillouin wave generated by the first section of the fiber. Therefore, the overall power spectral density of the backscattered Brillouin wave can be written as

$$\begin{aligned} S_{backward}(\omega) = & S_{BBW1}(\omega + \omega_c) + S_{BBW1}(\omega + \omega_c - 2\omega_s) + S_{BBW3}(\omega + \omega_c - 2\omega_s) \\ & + S_{BBW3}(\omega + \omega_c - 4\omega_s) \end{aligned} \tag{4}$$

where $S_{BBW1}(\omega)$ and $S_{BBW3}(\omega)$ are the spectrum of the backscattered Brillouin wave generated by the first and third section of the fiber, respectively. Note that both the first and third section of the fiber generate a backscattered Brillouin wave at $f_c - 2f_s$. Hence, this backscattered Brillouin wave has higher amplitude compared to that at f_c and $f_c - 4f_s$. This is verified experimentally and is showed in Fig. 9. The figure also shows the backscattered Brillouin wave at f_c has higher amplitude than that at $f_c - 4f_s$. The three backscattered Brillouin waves are amplified by the EDFA to above the single mode fiber SBS threshold value and are launched into the fourth section of the fiber via the

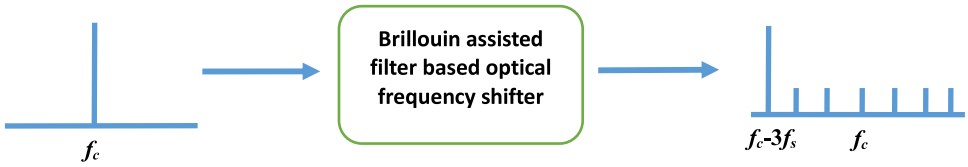

Fig. 4. Brillouin assisted filter based optical frequency shifter input and output spectrums.

second circulator. The backscattered Brillouin wave at f_c, $f_c - 2f_s$ and $f_c - 4f_s$ generate three sets of SBS gain and loss spectrums in the forward Stokes wave as shown in Fig. 3(d). Therefore, the power spectral density of the forward Stokes wave after passing through the fourth section of the fiber into Port 2 of the second optical circulator is given by

$$\begin{aligned} S_{out}(\omega) = \pi P_{in} t_{ff} e^{-\alpha 4L} \Bigg[& J_1{}^2(\beta_s) \frac{1}{g_{B1,2\omega_s}(\omega_c - \omega_s)} \frac{1}{g_{B2,2\omega_s}(\omega_c - \omega_s)} g_{B1}(\omega_c - \omega_s)\, \delta(\omega + \omega_c - \omega_s) \\ & + J_1{}^2(\beta_s) \frac{1}{g_{B1}(\omega_c + \omega_s)} \delta(\omega + \omega_c + \omega_s) \\ & + J_3{}^2(\beta_s)\, g_{B1,2\omega_s}(\omega_c - 3\omega_s)\, g_{B2,2\omega_s}(\omega_c - 3\omega_s) \\ & \cdot \frac{1}{g_{B2,4\omega_s}(\omega_c - 3\omega_s)} \delta(\omega + \omega_c - 3\omega_s) \\ & + J_3{}^2(\beta_s)\, \delta(\omega + \omega_c + 3\omega_s) \Bigg] \end{aligned} \tag{5}$$

where $g_{B2}(\omega)$, $g_{B2,2\omega s}(\omega)$ and $g_{B2,4\omega s}(\omega)$ are the SBS gain spectrums generated by the backscattered Brillouin waves at f_c, $f_c - 2f_s$ and $f_c - 4f_s$ into the fourth section of the fiber, respectively. Since the backscattered Brillouin wave at $f_c - 2f_s$ has higher amplitude compared to that at f_c and $f_c - 4f_s$, the peak value of the SBS gain spectrum $g_{B2,2\omega s}(\omega)$ is higher than that of $g_{B2}(\omega)$ and $g_{B2,4\omega s}(\omega)$. Similarly the dip of the SBS loss spectrum generated by the backscattered Brillouin wave at $f_c - 2f_s$ is deeper than that generated by the backscattered Brillouin waves at f_c and $f_c - 4f_s$, as shown in Fig. 3(d). Hence, the negative fundamental sideband, which aligned with the SBS gain and loss spectrum generated by the backscattered Brillouin wave at f_c and $f_c - 2f_s$ respectively, is attenuated after passing through the single mode fiber. It can be seen from (5) that the two fundamental sidebands are attenuated but the negative third order sideband is amplified. As a result, the laser frequency is shifted from f_c to the negative third order sideband frequency $f_c - 3f_s$ at the output of the Brillouin assisted filter. The input and output spectrum of the Brillouin assisted filter based optical frequency shifter are depicted in Fig. 4. Note that, in addition to the sidebands, the output of the optical frequency shifter also consists of the residual carrier due to the practical MZMs have limited extinction ratio, the Rayleigh backscattering components from the backward traveling wave and the SBS noise components at the center of the SBS gain spectrums. The amplitude of the input single frequency tone and the gain of the EDFA are designed to maximize the amplitude of the frequency shifted light while minimise the unwanted frequency components, the Rayleigh backscattering components and the SBS noise components.

Since the optical frequency shifter requires the frequency of the input electrical driving signal to be the same as the SBS frequency of the Brillouin medium and the SBS frequency of a normal single mode fiber is around 11 GHz at 1.55 μm [11], the amount of frequency shift that can be obtained by the Brillouin assisted filter based optical frequency shifter is around 33 GHz. This shows 33 GHz optical frequency shift can be obtained using an 11 GHz electrical driving signal. Reducing the electrical driving signal frequency can lower the system cost, which is the advantage of the new optical frequency shifter compared to all the reported optical frequency shifters [4]–[7] that require the electrical driving signal frequency to be the same as the frequency shift. Altering the

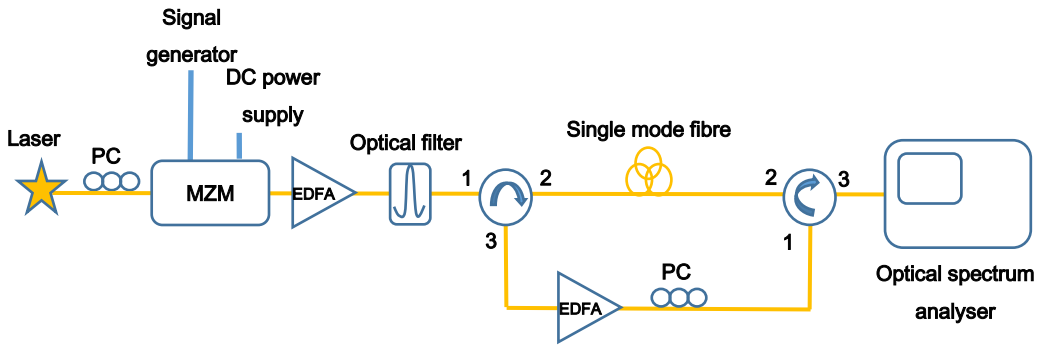

Fig. 5. Experimental setup of the Brillouin assisted filter based optical frequency shifter.

wavelength of the incident light can change the single mode fiber Brillouin frequency [16], which in turn enables continuous tuning the frequency shift via controlling the electrical driving signal frequency. However, this technique can only change the 33 GHz frequency shift by several hundred MHz. Different fibers, which have different Brillouin frequencies, can be used as a Brillouin medium in the Brillouin assisted filter to obtain different optical frequency shifts. For example, a polymer chalcogenide tapered fiber has a Brillouin frequency of 6.8 GHz and can be increased to 8.15 GHz by altering the fiber core diameter [17]. Hence a frequency shift ranges from 20.4 GHz to 24.45 GHz can be obtained using this fiber. Our previous work on optical frequency shifters is based on designing the frequency of the pump wave for the SBS process to be the difference between the Stokes wave frequency and the SBS frequency of the Brillouin medium [7]. This requires two minimum-biased MZMs where one MZM is driven by a single tone with the frequency equal to the amount of frequency shift and is used to generate the Stokes wave. The other MZM is driven by another single tone with the frequency equal to the difference between the frequency shift and the SBS frequency, and is used to generate the pump wave. The use of two MZMs and two microwave signal generators increases the size and cost of the system. This precludes the SBS based optical frequency shifter to be used in practice. The new optical frequency shifter presented in this paper overcomes the problem by employing a Brillouin assisted filtering structure in which the backscattered Brillouin wave from the Brillouin medium is used as the pump wave for the SBS process. Hence only one MZM and one microwave signal generator are needed. Furthermore, the experimental results presented in the following section show the Brillouin assisted filter based optical frequency shifter has over 9 dB signal-to-noise ratio improvement compared to the previously reported optical frequency shifter [7]. Note that the Brillouin assisted filter based optical frequency shifter does not involve electrical components. It is low cost compared to other optical frequency shifting structures since the frequency of the electrical driving signal only needs to be one third of the frequency shift.

3. Experimental Results

Experiments were conducted to verify the concept of the new optical frequency shifter. The experimental setup is shown in Fig. 5. A laser source generated a continuous wave light with 1551.016 nm wavelength (or 193.2878 THz frequency) and 1.2 dBm optical power, which were measured by an optical spectrum analyzer (OSA) with 0.03 nm resolution bandwidth. The light was modulated in a MZM, which had 30.6 dB extinction ratio. A DC voltage of 3.3 V from a DC power supply was applied to the MZM to bias the modulator at the minimum transmission point. Due to the lack of a high power signal generator, an electrical amplifier was used to amplify a single frequency tone from a signal generator to 25.6 dBm. A polarization controller (PC) in front of the MZM was used to align the light polarization state into the MZM. The fundamental RF modulation sidebands at the output of the MZM were amplified by an EDFA to above the SBS

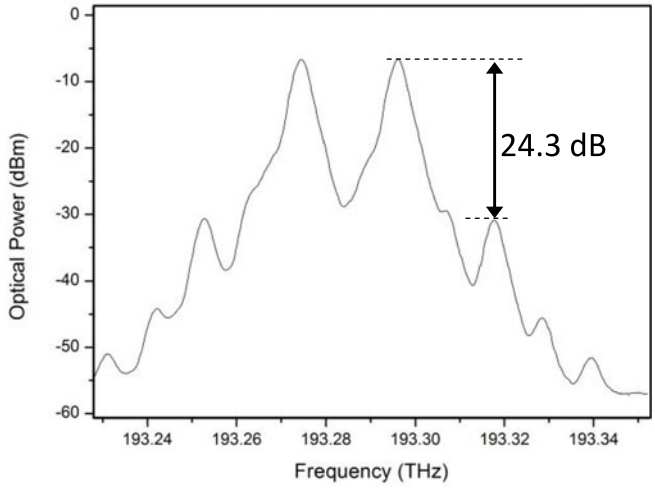

Fig. 6. Optical spectrum of the DSB-SC RF modulated optical signal into the Brillouin assisted filter. The single tone frequency into the MZM was 10.842 GHz.

threshold value of the optical fiber inside the Brillouin assisted filter. The amplified spontaneous emission noise generated by the EDFA was suppressed by an optical filter with a center wavelength of 1551.02 nm and a 3 dB passband width of 1.12 nm or 140 GHz. This enables all the sidebands up to and including the 6th order sidebands at the MZM output to pass through the optical filter with only small attenuation due to the optical filter insertion loss. The 7th and the higher order sidebands were outside the optical filter passband and were suppressed by the optical filter. However, they have very small power since the power of the n^{th} order sideband is proportional to $J_n(\beta_s)^2$. Hence, they can be neglected even without the presence of the optical filter. Note that the EDFA and the optical filter can be avoided by using a high power laser source. The spectrum of the DSB-SC RF modulated optical signal at the optical filter output was measured on the OSA with a 15 dB attenuation attenuator at the input to avoid saturation and is depicted in Fig. 6. It can be seen from the figure that the carrier was suppressed and the fundamental sidebands were 24.3 dB above the third order sidebands. The Brillouin assisted filter was implemented by a 25.3 km single mode fiber between a pair of optical circulators. The single mode fiber, which acted as a Brillouin medium, had a Brillouin frequency of 10.842 GHz at 1551.016 nm and a Brillouin linewidth of 10 MHz. The power of the backscattered Brillouin wave was measured at Port 3 of the first circulator for different fundamental sideband powers. Fig. 7 shows the power of the backscattered Brillouin wave was saturated at around –7 dBm, which cannot be further increased by increasing the fundamental sideband power. This indicates that an EDFA inside the Brillouin assisted filter is needed to amplify the backscattered Brillouin wave to above the single mode fiber SBS threshold value.

The EDFA gain was adjusted to maximize the amplitude of the frequency shifted light while minimise the unwanted frequency components. The relative polarization state between the forward and backward traveling wave into the single mode fiber was controlled by a PC at Port 1 of the second circulator. The PC was adjusted to maximize the output frequency shifted light amplitude. The frequency shifted light was measured at Port 3 of the second circulator using the OSA with 0.03 nm resolution bandwidth. Fig. 8 depicts the spectrum at the output of the Brillouin assisted filter based optical frequency shifter when the frequency of the single tone into the MZM was set to be the Brillouin frequency of the single mode fiber used in the experiment, i.e. 10.842 GHz. The laser output spectrum is also shown in the figure for comparison. The measurements show 32.53 GHz down shift in the laser frequency from 193.2878 THz to 193.2553 THz. This demonstrates the frequency shifting operation and the amount of frequency shift is three times the input single

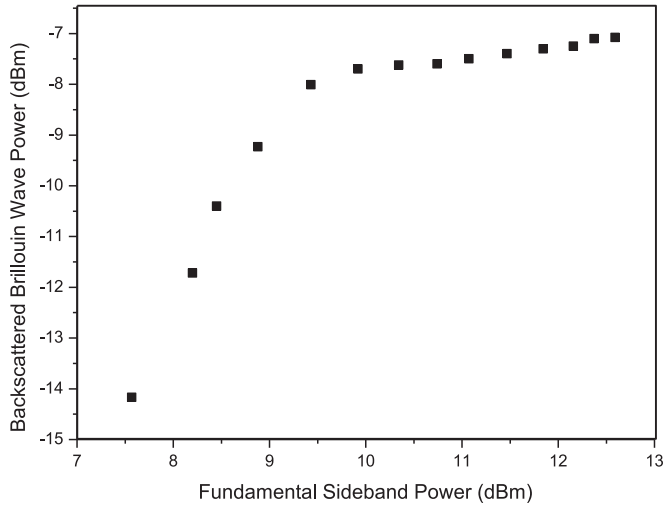

Fig. 7. Backscattered Brillouin wave power as a function of the power of the fundamental sideband into the Brillouin assisted filter.

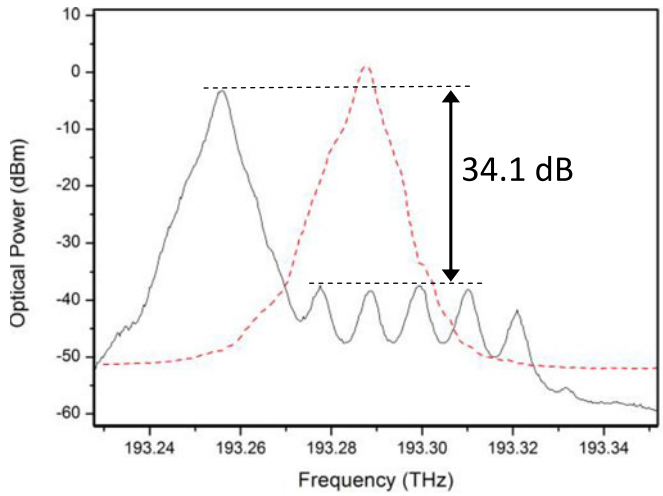

Fig. 8. Measured input (dotted) and output (solid) spectrums of the Brillouin assisted filter based optical frequency shifter.

tone frequency. Fig. 8 shows the two fundamental sidebands at 193.2776 THz and 193.2993 THz are the highest unwanted frequency components and they are 34.1 dB below the frequency shifted light. To the best of our knowledge, this is the highest reported frequency shifted to unwanted frequency component ratio for a large frequency shift of above 30 GHz. Fig. 8 also shows the unwanted frequency components at the optical frequency shifter output consists of the residual carrier at 193.2878 THz, the sidebands that cannot be fully eliminated by the SBS loss spectrums, the SBS noise components, and the Rayleigh backscattering components. Note that the unwanted frequency component at 193.3102 THz, which is the second order sideband, is due to the second order harmonic component generated by the electrical amplifier at the modulator input. Using a high power signal generator can avoid the electrical amplifier, which in turn reduces the unwanted second order sidebands at the frequency shifter output. The backward traveling wave, i.e. the pump wave, into the single mode fiber in order to shift the light frequency as shown in Fig. 8 was measured by inserting a 50% coupling ratio optical coupler at Port 2 of the second circulator. Again, a 15 dB

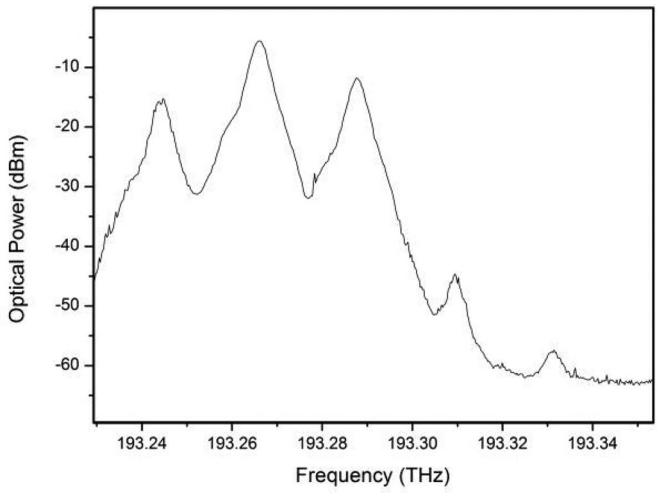

Fig. 9. Backward traveling wave at Port 2 of the second optical circulator.

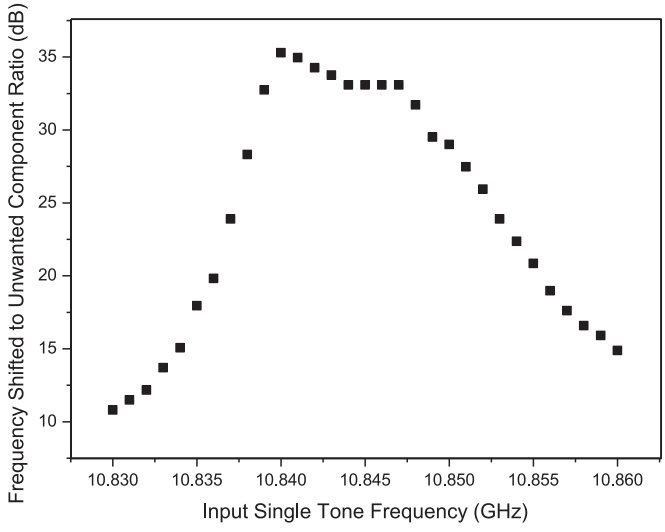

Fig. 10. Frequency shifted to unwanted frequency component ratio for different frequency input single tone into the modulator.

attenuation attenuator at the OSA input was used to avoid saturation. Fig. 9 shows the spectrum of the backward traveling wave. It can be seen that the backscattered Brillouin wave at 193.2661 THz, which corresponds to the frequency $f_c - 2f_s$, has higher amplitude compared to that at 193.2878 THz and 193.2447 THz, which correspond to the frequencies f_c and $f_c - 4f_s$, respectively. They generate three sets of gain and loss spectrums with different amplitudes in the forward traveling wave as they pass through the single mode fiber. This results in the amplification in one of the third order sidebands and attenuation in the other sidebands of the input DSB-SC RF modulated optical signal.

The ratio of the frequency shifted to unwanted frequency components for different electrical driving signal frequency, while fixing the laser wavelength at 1551.016 nm, was investigated experimentally. Fig. 10 shows a high frequency shifted to unwanted frequency component ratio of over 30 dB can be maintained when the electrical driving signal frequency was changed from 10.838 GHz to 10.849 GHz. This enables the optical frequency shift to be tuned from 32.514 GHz to 32.547 GHz.

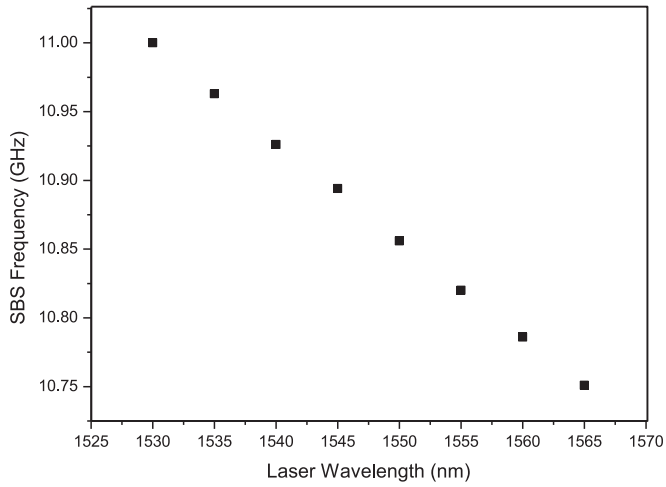

Fig. 11. Single mode fiber SBS frequency versus laser source wavelength.

A larger optical frequency shift tuning is expected by using the phase modulation technique [18] to broaden the Brillouin linewidth. Another way to tune the frequency shift over a wide frequency range is to alter the SBS frequency of the Brillouin medium by changing the laser source wavelength. The SBS frequency of the single mode fiber used in the experiment was measured for different laser wavelengths. Fig. 11 shows a linear relationship between the SBS frequency and the laser wavelength, and 249 MHz changes in the SBS frequency can be obtained by tuning the laser wavelength from 1530 nm to 1565 nm. Shifting the laser frequency by three times the single mode fiber SBS frequency with a large frequency shifted to unwanted frequency component ratio was demonstrated experimentally for different laser wavelengths. The results show the optical frequency shift can be tuned over 747 MHz frequency range for 35 nm changes in the laser wavelength. It should be pointed out that an optical frequency shifter can be inserted anywhere in an optical system to alter the frequency of its input optical signal. This is different compared to a wavelength tunable laser that controls the frequency or wavelength of a continuous wave light at the tunable laser output. Furthermore, in applications such as a SBS based microwave photonic bandpass filter [19] and a coherence-free microwave photonic notch filter [20], two continuous wave light with a fixed frequency separation are needed. Using two tunable laser sources increases the system cost and most importantly the frequency separation between the two continuous wave light cannot be fixed but is changing with time due to slight fluctuation in the tunable laser wavelengths. This in turn causes fluctuation in the SBS based microwave photonic bandpass filter response [19]. Splitting the output of a laser source into two where one is connected to an optical frequency shifter provides a solution to this problem.

4. Conclusion

A new optical frequency shifter has been presented. It is based on SBS in a single mode fiber inside a Brillouin assisted filtering structure that generates multiple SBS gain and loss spectrums to amplify a third order sideband but attenuate other sidebands. The Brillouin assisted filter based optical frequency shifter has the advantages of not only capable of realizing a large frequency shift but also the electrical driving signal frequency only needs to be one third of the frequency shift. This reduces the system cost compared to all the reported optical frequency shifters that require an electrical driving signal to have the same frequency as the frequency shift. The optical frequency shifter has a simple structure and can be implemented using off-the-shelf optical components. The Brillouin assisted filter based optical frequency shifter has been demonstrated experimentally with the results showing a large 32.53 GHz frequency shift with over 34 dB frequency shifted to

unwanted frequency component ratio. Tuning the frequency shift by controlling the laser frequency and the electrical driving signal frequency has also been demonstrated.

References

[1] H. E. Engan, B. Y. Kim, J. N. Blake, and H. J. Shaw, "Optical frequency shifting in two-mode optical fibers by flexural acoustic waves," in *Proc. IEEE Ultrason. Symp.*, 1986, pp. 435–438.

[2] I. Y. Poberezhskiy, B. Bortnik, J. Chou, B. Jalali, and H. R. Fetterman, "Serrodyne frequency translation of continuous optical signals using ultrawide-band electrical sawtooth waveforms," *IEEE J. Quantum Electron.*, vol. 41, no. 12, pp. 1533–1539, Dec. 2005.

[3] M. G. Gazalet, M. Ravez, F. Haine, C. Bruneel, and E. Bridoux, "Acousto-optic low-frequency shifter," *Appl. Opt.*, vol. 33, no. 7, pp. 1293–1298, 1994.

[4] W. Chujo, T. Hanasaka, M. Naganuma, and T. Yoneyama, "A 60-GHz optical frequency shifter using coupled inverted slot lines," *IEEE Trans. Microw. Theory Tech.*, vol. 47, no. 12, pp. 2280–2286, Dec. 1999.

[5] M. Y. Frankel and R. D. Esman, "Optical single-sideband suppressed-carrier modulator for wide-band signal processing," *J. Lightw. Technol.*, vol. 16, no. 5, pp. 859–863, May 1998.

[6] K. Higuma, S. Oikawa, Y. Hashimoto, H. Nagata, and M. Izutsu, "X-cut lithium niobate optical single-sideband modulator," *Electron. Lett.*, vol. 37, no. 8, pp. 515–516, 2001.

[7] E. H. W. Chan and R. A. Minasian, "All-optical frequency shifter based on stimulated Brillouin scattering in an optical fiber," *IEEE Photon. J.*, vol. 6, no. 2, Apr. 2014, Art. no. 6600210.

[8] W. Li and J. Yao, "Investigation of photonically assisted microwave frequency multiplication based on external modulation," *IEEE Trans. Microwave Theory Tech.*, vol. 58, no. 11, pp. 3259–3268, Nov. 2010.

[9] G. H. Smith, D. Novak, and Z. Ahmed, "Overcoming chromatic-dispersion effects in fiber-wireless systems incorporating external modulators," *IEEE Trans. Microw. Theory Tech.*, vol. 45, no. 8, pp. 1410–1415, Aug. 1997.

[10] B. Chen, S. Zheng, H. Chi, X. Zhang, and X. Jin, "An optical millimeter-wave generation technique based on phase modulation and Brillouin-assisted notch-filtering," *IEEE Photon. Technol. Lett.*, vol. 20, no. 24, pp. 2057–2059, Dec. 2008.

[11] A. Loayssa, D. Benito, and M. J. Garde, "Applications of optical carrier Brillouin processing to microwave photonics," *Opt. Fiber Technol.*, vol. 8, no. 1, pp. 24–42, 2002.

[12] M. Horowitz, A. R. Chraplyvy, R. W. Tkach, and J. L. Zyskind, "Broad-band transmitted intensity noise induced by stokes and anti-stokes Brillouin scattering in single-mode fibers," *IEEE Photon. Technol. Lett.*, vol. 9, no. 1, pp. 124–126, Jan. 1997.

[13] R. B. Jenkins, R. M. Sova, and R. I. Joseph, "Steady-state noise analysis of spontaneous and stimulated Brillouin scattering in optical fibers," *J. Lightw. Technol.*, vol. 25, no. 3, pp. 763–770, Mar. 2007.

[14] A. Yeniay, J. M. Delavaux, and J. Toulouse, "Spontaneous and stimulated Brillouin scattering gain spectra in optical fibers," *J. Lightw. Technol.*, vol. 20, no. 8, pp. 1425–1432, Aug. 2002.

[15] L. Yi, T. Zhang, Z. Li, J. Zhou, Y. Dong, and W. Hu, "Secure optical communication using stimulated Brillouin scattering in optical fiber," *Opt. Commun.*, vol. 290, pp. 146–151, 2013.

[16] M. Nikles, L. Thevenaz, and P. A. Robert, "Brillouin gain spectrum characterization in single-mode optical fibers," *J. Lightw. Technol.*, vol. 15, no. 10, pp. 1842–1851, Oct. 1997.

[17] J. C. Beugnot, R. Ahmad, M. Rochette, V. Laude, H. Maillotte, and T. Sylvestre, "Tunable stimulated Brillouin scattering in hybrid polymer-chalcogenide tapered fibers," *Proc. SPIE*, vol. 9136, 2014, Art. no. 91360O.

[18] T. A. Nguyen, E. H. W. Chan, and R. A. Minasian, "Instantaneous high-resolution multiple frequency measurement system based on frequency-to-time mapping technique," *Opt. Lett.*, vol. 39, no. 8, pp. 2419–2422, 2014.

[19] M. Pagani, E. H. W. Chan, and R. A. Minasian, "A study of the linearity performance of a stimulated Brillouin scattering based microwave photonic bandpass filter," *J. Lightw. Technol.*, vol. 32, no. 5, pp. 999–1005, Mar. 2014.

[20] E. H. W. Chan, "Coherence-free optical delay line signal processor," *Electron. Lett.*, vol. 43, no. 17, pp. 947–948, 2007.